

S-wave superconductivity with orbital dependent sign change in the checkerboard models of iron-based superconductors

Xiaoli Lu,^{1,2} Chen Fang,² Wei-Feng Tsai,³ Yongjin Jiang,^{1,2} and Jiangping Hu^{2,4,*}

¹Center for Statistical and Theoretical Condensed Matter Physics,
and Department of Physics, Zhejiang Normal University, Jinhua 321004, China

²Department of Physics, Purdue University, West Lafayette, Indiana 47907, USA

³Institute for Solid State Physics, University of Tokyo, Kashiwa 277-8581, Japan

⁴Beijing National Laboratory for Condensed Matter Physics,
Institute of Physics, Chinese Academy of Sciences, Beijing 100080, China

We study three different multi-orbital models for iron-based superconductors (iron-SCs) in the solvable limit of weakly coupled square plaquettes. The strongest superconducting (SC) pairing is in the A_{1g} s -wave channel and its development is correlated with the emergence of the next-nearest-neighbour antiferromagnetism (NNN-AFM). For the models with more than three orbitals, this study suggests that the signs of the intra-orbital pairing order parameters of the d_{xy} and the d_{xz} (or d_{yz}) orbitals must be *opposite*. Such sign difference stems from the intrinsic symmetry properties of inter-orbital hoppings and might, ultimately, lead to the sign-change of the SC orders between the hole Fermi pockets at the Γ point and produce anisotropic or even gapless SC gaps in the electron Fermi pockets around the M point in reciprocal space, as restoring back to the homogeneous limit.

Introduction.— Since the iron-based superconductors were discovered two years ago[1], the relation between the new superconductors and the high- T_c cuprates has been a central focus of researches. It is highly debated that whether the new superconductors belong to the same category of strongly correlated electron systems in which the cuprates are believed to be. Models based on both strong coupling [2–9] and weak coupling[10–16] approaches have been applied to understand the properties of the new materials and their relation to the cuprates.

Strong correlation in an electron system can be reflected in its strong “locality” of physical properties caused by short-range interactions. For instance, both magnetism and superconductivity in the cuprates could be attributed to such “local” physics. The magnetism in the parent cuprate compounds is well described by the Heisenberg model with the nearest-neighbor (NN) antiferromagnetic (AFM) exchange couplings. The d -wave superconductivity with symmetry form factor, $\cos k_x - \cos k_y$, in reciprocal space[17] corresponds to short-range superconducting (SC) pairings between just the NN copper sites. Theoretically, the locality (short coherence length) already allows us to understand many essential physics from small clusters and to give new insights for obtaining low-energy effective models[18–21].

Remarkably, recent experimental results in iron-based superconductors suggest that both magnetism and superconductivity display an excellent locality behavior as well. Neutron scattering experiments demonstrate that the magnetism in the parent compounds of iron-SCs can be again described well by the Heisenberg model with the NN and the NNN-antiferromagnetic exchange couplings between iron spins[22–24]. In addition, angle resolved photo emission spectroscopy (ARPES) experiments show that the SC gaps can be fitted to a single $\cos k_x \cos k_y$ functional form in reciprocal space[25–27]. Regarding

the fact that iron-SCs are complicated multi-orbital systems, these experimental results are compelling evidence supporting that a local interaction controls the pairing channels since the function form in the real space simply corresponds to SC pairings between the NNN iron sites. They motivate us to ask whether the physics of iron-SCs can also be understood from checkerboard-like models as studied in Ref. [19], where the local physics (within a plaquette) can be solved exactly, with an assumption that the major physics would remain unchanged as the models are adiabatically tuned to the homogeneous limit.

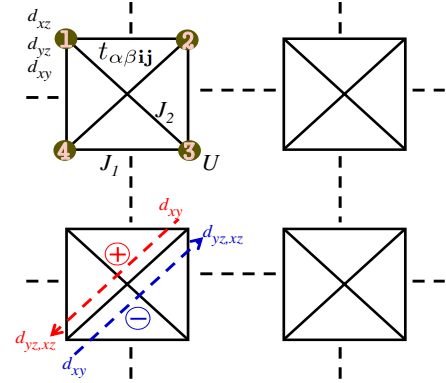


FIG. 1: The sketch of the checkerboard models. The hopping signs between d_{xy} and $d_{xz(yz)}$ orbitals are indicated.

In this Letter, we present results for three different tight-binding models for iron-SCs which are constructed using two [28], three [29], and four orbitals[30], respectively, on a checkerboard lattice (see Fig. 1). Based on the knowledge of exactly solvable four-site problems, we show the phase diagrams of the models in the limit of weakly coupled plaquettes as a function of intra-orbital onsite interaction U , inter-orbital onsite interaction U' ,

Hund's coupling and onsite inter-orbital pairing hopping J_H , as well as the NNN-AFM coupling J_2 which can be generated by superexchange mechanism mediated by As atoms. In all of the models, the leading SC phase is always from the A_{1g} s -wave pairing channel in reasonable parameter regions. The superconductivity is intimately correlated with the development of the NNN-AFM and becomes stronger as J_2 increases. Most remarkably, this study also shows that the superconductivity and magnetism are orbital-selective in the three- and four-orbital models: First, in the three-orbital model, the AFM is more pronounced in the d_{xy} orbital while the superconductivity is more pronounced in the d_{xz} and d_{yz} orbitals. Second, in both three- and four-orbital models, the signs of the intra-orbital pairing order parameters of the d_{xy} and the d_{xz} (or d_{yz}) orbitals are opposite. The sign difference stems from the intrinsic symmetry of the inter-orbital hopping amplitudes between d_{xy} and $d_{xz(yz)}$ [32]. This feature could result in the sign-change of the SC order parameters between the hole Fermi pockets at the Γ point and produce anisotropic or gapless SC gaps in the electron pockets around M point in reciprocal space in the homogeneous limit.

Model and method.- A generic Hamiltonian of iron-SCs can be written as $H = H_0 + H_I$, where H_0 is the kinetic energy of the d -electrons of irons and H_I describes the interactions between them. Explicitly, H_0 is given by

$$H_0 = \sum_{\mathbf{i}, \mathbf{j}, \sigma} \sum_{\alpha, \beta} (t_{\alpha\beta}^{\mathbf{i}\mathbf{j}} + \epsilon_{\alpha} \delta_{\alpha\beta}) d_{\mathbf{i}, \alpha, \sigma}^{\dagger} d_{\mathbf{j}, \beta, \sigma} + H.c. \quad (1)$$

where α, β are orbital indices, \mathbf{i}, \mathbf{j} label sites and σ is spin index. H_I can be written as $H_I = \sum_i H_{I_o}(i) + H_{I_e}$, where $H_{I_o}(i)$ is the onsite interaction, given by,

$$H_{I_o}(\mathbf{i}) = U \sum_{\alpha} n_{\mathbf{i}, \alpha, \uparrow} n_{\mathbf{i}, \alpha, \downarrow} + \sum_{\alpha \neq \beta} \left[\frac{U'}{2} n_{\mathbf{i}, \alpha} n_{\mathbf{i}, \beta} - \frac{J_H}{2} S_{i\alpha} S_{i\beta} \right] + J \sum_{\alpha \neq \beta} d_{\mathbf{i}, \alpha, \uparrow}^{\dagger} d_{\mathbf{i}, \alpha, \downarrow}^{\dagger} d_{\mathbf{i}, \beta, \downarrow} d_{\mathbf{i}, \beta, \uparrow}, \quad (2)$$

with U , U' , J_H , and $J(= J_H)$ denoting intra-orbital repulsion, inter-orbital repulsion, ferromagnetic Hund's coupling, and inter-orbital pair hopping, respectively. H_{I_e} describes interactions between different sites. In this paper, we specifically consider the NNN (denoted by double angle brackets) magnetic exchange coupling J_2 , which can be naturally generated by the superexchange mechanism through As atoms,

$$H_{I_e} = \sum_{\langle\langle \mathbf{i}, \mathbf{j} \rangle\rangle} \sum_{\alpha, \beta} J_2 \mathbf{S}_{\mathbf{i}, \alpha} \cdot \mathbf{S}_{\mathbf{j}, \beta}. \quad (3)$$

Different tight-binding models have been proposed to describe the band structures of iron-SCs. In this study, we take three different models: a two-orbital model given in [28], a three-orbital model given in [29], and a four-orbital model in [30]. The tight-binding parameters of

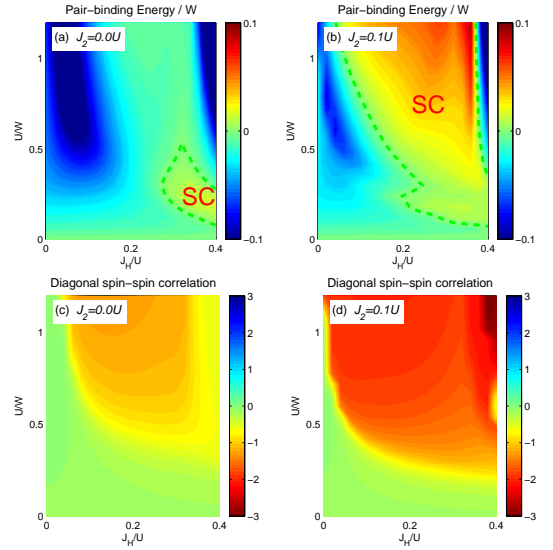


FIG. 2: The pair-binding energy [(a) and (b)] and the diagonal spin-spin correlations [(c) and (d)] for 2×2 plaquette in the three-orbital model are plotted as functions of U/W and J_H/U with [(a) and (c)] and without [(b) and (d)] exchange coupling J_2 . The dotted lines in (a) and (b) enclose the regions with positive pair-binding energy, suggesting a SC phase.

the models can be found in the above references. We have also tried different four-orbital models reduced from the five-orbital models constructed in[11]. All of the models capture the basic band structures of iron-SCs. In fact, the major results reported below are consistent in all of these models.

The checkerboard models are defined on the lattice shown in Fig. 1, with the inter-plaquette hopping amplitudes $\tau_{\alpha\beta}^{ij}$ and exchange couplings \mathcal{J}_2 less than intra-plaquette parameters, $t_{\alpha\beta}^{ij}$ and J_2 . A four-site plaquette can be diagonalized exactly, though one may necessarily resort to the numerics due to its multi-orbital complexity. Consequently, we can determine the pair-binding energy $E_p = 2E(1) - E(0) - E(2)$, where $E(Q)$ is the ground-state energy for a given Q , the number of doped holes in an “undoped” reference state. In particular, $E_p > 0$ indicates an effective attraction between doped holes. At generic doping, we consider the case $0 \leq \{\tau_{\alpha\beta}^{ij}, \mathcal{J}_2\} \ll E_p \ll \{t_{\alpha\beta}^{ij}, J_2\}$, which allows us to obtain a controlled perturbation expansion of the full Hamiltonian by small inter-plaquette parameters. Second order perturbation gives us an effective theory describing interacting bosons ($Q = 2$ states) with hopping integrals and short-range density-density interactions of order τ^2/E_p on the effective lattice. Furthermore, it can be proved that the ground state enters superfluidity at $T = 0$ [31], except at special doping percentages. Thus, the positiveness of E_p could be used as an economic way to identify SC phase with generic doping.

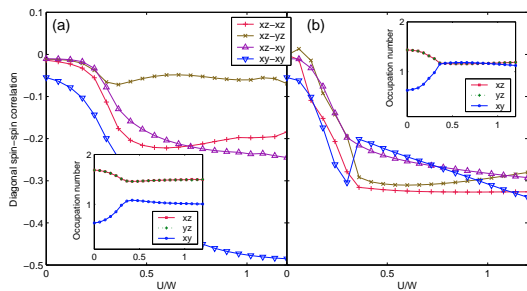


FIG. 3: The orbital-resolved diagonal spin-spin correlations, $\langle \mathbf{S}_\alpha^1 \cdot \mathbf{S}_\beta^3 \rangle$ ($\alpha, \beta = xz, yz, xy$), of a 2×2 cluster with 16 electrons ($2/3$ filling) (a) and 14 electrons (b). The parameters are given by $J_H = 0.2U$, $J_2 = 0.1U$. Insets: The occupation number of different orbitals as a function of U/W with 16 electrons and 14 electrons, respectively.

Spin and pairing correlations.— The two-orbital model consists of the d_{xz} and d_{yz} orbitals and has been studied both analytically and numerically due to its simplicity. However, there is no SC phase in the physically meaningful parameter region in our study if $J_2 = 0$. This sharp feature is very similar to the results obtained from the functional renormalization group (fRG) for such a model[13], although the fRG is, in principle, a weak-coupling approach. When J_2 is added, the superconductivity and magnetism in these two orbitals behave no qualitative difference from those in three- and four-orbital models within the same orbitals. Therefore, we will focus on reporting the results from the three- and four-orbital models hereafter.

We summarize the main results for the three-orbital model in Figs. 2, 3, and 4. Note that the parent compounds here refer to $2/3$ filling, instead of $1/2$ filling in two- and four-orbital models. In Fig. 2, we plot the pair-binding energy and the diagonal (NNN) spin-spin correlation function as a function of U/W and J_H/U with U' satisfying the $SU(2)$ symmetry condition $U' = U - 2.5J_H$ and W being the bandwidth. As shown in the figure, without J_2 , there is a small region (circled by the dash line) where the SC state is favored and this region is located within the region the NNN-AFM is developed. With a finite $J_2 = 0.1U$, the SC region is significantly enlarged as well as the NNN-AFM correlation. It is also important to note that a finite J_H is needed in order to achieve positive pair-binding energy.

The NNN spin-spin correlation within a plaquette, $\langle Q; \text{GS} | \mathbf{S}_\alpha^1 \cdot \mathbf{S}_\beta^3 | Q; \text{GS} \rangle$, as a function of U/W is shown in Fig. 3 with fixed $J_H = 0.2U$ and $J_2 = 0.1U$. The NNN-AFM correlation develops when U reaches close to $0.4W$ and the intra-orbital correlations are much stronger than the inter-orbital correlations. Moreover, the d_{xy} orbital has the strongest NNN-AFM correlation as expected since the d_{xy} orbital is half filled [see Inset of Fig. 3(a)]. After doping two holes per plaquette, the

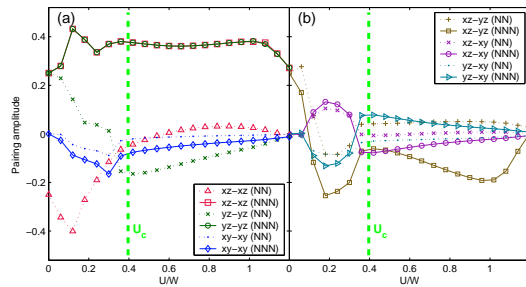


FIG. 4: The pairing amplitude of the intra-orbital (a) and the inter-orbital (b) electron pairs as function of U at fixed parameters of $J_H = 0.2U$ and $J_2 = 0.1U$. The green dotted lines divide the regions of positive (right) and negative (left) pairing energy. The ‘NN’ in the legend means sites 1&2 while ‘NNN’ means sites 1&3; all other pairings’ amplitude can be derived from the A_{1g} symmetry.

correlations become even among all the orbitals, as suggested by equally distributed occupation number among all orbitals [see Inset of Fig. 3(b)].

The SC pairing amplitudes, defined as $\langle Q = 2; \text{GS} | \Delta_{\alpha\beta}(\mathbf{ij}) | Q = 0; \text{GS} \rangle$ with $\Delta_{\alpha\beta}(\mathbf{ij}) = d_{i,\alpha,\downarrow} d_{j,\beta,\uparrow} - d_{i,\alpha,\uparrow} d_{j,\beta,\downarrow}$, are shown in Fig. 4. The positive pair-binding energy is achieved when $U > U_c \sim 0.4W$, close to where the NNN-AFM has well developed. As $E_p > 0$, it is important to notice that due to C_{4v} symmetry of a single plaquette and the fact $|Q = 0; \text{GS}\rangle, |Q = 2; \text{GS}\rangle$ belonging to A_{1g} representation, the pair-field operator must have precisely A_{1g} s -wave symmetry. The intra-orbital NNN pairings in the $d_{xz(yz)}$ orbitals dominate the pairing strength. The pairing in the d_{xy} orbital is small since the d_{xy} orbital remains half-filled and its AFM correlation is too strong. However, this is an important feature that even as the pairing strength is small in the d_{xy} orbital, the sign of the pairing is opposite to the ones in the $d_{xz(yz)}$ orbitals. We find that the sign-change is as universal as the A_{1g} s -wave pairing symmetry in all of the parameter regions we calculate.

The above major results still hold in the four-orbital model as summarized in Fig. 5(a). The pairing symmetry is still A_{1g} s -wave and with a sign change between the d_{xy} and $d_{xz(yz)}$ orbitals. As shown in Fig. 5(a), the positive pairing energy is achieved when U reaches about $0.4W$ as well. The NN-AFM is relatively stronger in the four orbital model than the one in the three-orbital model since the NNN hopping is weaker. The SC pairing in the fourth orbital $d_{x^2-y^2}$ is negligible, while the SC pairing strength in the d_{xy} orbital becomes stronger, compared to the three-orbital model.

To understand the signs of SC order parameters of different orbitals, we can consider the effective Josephson coupling between them. The Josephson couplings can be derived from inter-orbital hoppings. Let’s consider the inter-orbital hopping between arbitrary two sites (denoted by A and B) described by $H_h = t_{\alpha\beta}^{AB} (d_{A,\beta,\sigma}^\dagger d_{B,\alpha,\sigma} +$

H.c.), where α, β are two different orbitals. Assuming it is half-filled for both orbitals at the two sites and the spin singlet is formed within each orbital due to the intra-orbital AFM coupling between two sites, we can easily show the inter-orbital hopping can generate the effective Josephson coupling between two orbitals given by

$$H^{eff} = -2 \frac{t_{\alpha\beta}^{AB} t_{\beta\alpha}^{AB}}{U'} \Delta_{\alpha}^{\dagger} \Delta_{\beta}, \quad (4)$$

where Δ_{α} are the SC order parameters. In the case of iron-based superconductors, the general symmetry of the lattice requires $t_{xz,yz}^{ij} = t_{yz,xz}^{ij}$ and $t_{xy,xz(yz)}^{ij} = -t_{xz(yz),xy}^{ij}$, as sketched in Fig. 1. Thus the Josephson coupling between the xz and yz is negative while the one between the $xz(yz)$ and xy is positive, which favors the sign change between $\Delta_{xz(yz),xz(yz)}(ij)$ and $\Delta_{xy,xy}(ij)$. This explains the numerical results.

Discussion.- It is very interesting to compare our study to other previous theoretical studies. First, our study confirms that the pairing symmetry is dominated by the A_{1g} s -wave induced by the NNN-AFM coupling, which will lead to the sign change between electron and hole pockets as many previous studies have concluded[2, 4, 12, 13]. Second, our study suggests that the Hund's coupling is also important in inducing the SC pairing and the NNN-AFM correlation[7]. Without the Hund's coupling, the model does not lead to the SC instability. Third, our study indicates the importance of the d_{xy} orbital in the strong coupling limit. The pairing in the d_{xy} orbital favors an opposite sign to those in the d_{yz} and d_{xz} orbitals. This result, if still holds in the homogeneous limit, may also cause an anisotropic SC gap in the electron pockets at the M point of reciprocal space since the electron pockets include both the d_{xy} and $d_{xz(yz)}$ orbitals. The presence of d_{xy} can change many important properties of the SC pairing. Indeed, the importance of d_{xy} orbital has been emphasized in the weak coupling approaches, such as the fRG which shows that in the absence of the hole Fermi pocket from d_{xy} , an anisotropic gap can be developed, similar to our implication. However, the physical mechanism, as discussed earlier, is completely different from the one in a weak coupling approach. Finally, it is worth mentioning that the signs of the Josephson couplings obtained in eq.4 explain why the SC state with time reversal symmetry (TRS) breaking as suggested in [33, 34] for iron-SCs is not favored. A TRS broken state is favored if and only if the couplings between all three orbitals are positive.

Our study provides a new picture of the SC order parameters. In the context of iron-SCs, the A_{1g} s -wave pairing is generally agreed to exhibit the sign-change between electron and hole Fermi pockets via spin fluctuations. However, our study, though from inhomogeneous limit, suggests that in the presence of the d_{xy} orbital, there is an additional sign-change between the d_{xy} and

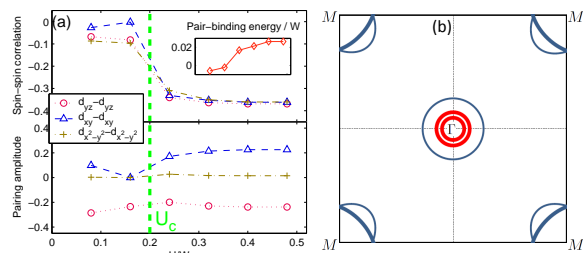


FIG. 5: **a:** The spin correlation (upper) and pairing amplitude (lower) of diagonal bonds as functions of U in the four-orbital model. The inset shows the pair binding energy in unit of band width. **b:** The schematic pairing amplitude of a 2D five-orbital model in the superconducting state inside the first (folded) Brillouin zone. Red and blue means positive and negative signs, and the thickness indicates the size of the gap.

the $d_{xz(yz)}$ orbitals. Considering the recent ARPES experiments, the large hole pocket at the Γ point is mainly from d_{xy} orbital while the small two hole pockets which are almost doubly degenerated is composed of the d_{xz} and d_{yz} orbitals[35]. Keeping these orbital characters in mind, our results do provide a testable, experimental prediction: the signs in SC order parameters are *opposite* for the large and small hole pockets at the Γ point. We present a schematic plot for SC order parameters in reciprocal space in Fig. 5(b). More physical consequences associated with such a sign change will be explored in the future study.

We thank A. B. Bernevig, S. Kivelson, H. Ding, D.L. Feng, X.H. Chen and P.C. Dai for help in discussion. JPH thanks E. Demler for asking question related to this study. YJJ acknowledge the support from NSF, Zhejiang (No.Y7080383) and NSF, China (No.11004174).

* Corresponding author; Electronic address: hu4@purdue.edu

- [1] Y. Kamihara, *et al*, J. Am. Chem. Soc. **130**, 3296 (2008).
- [2] K. Seo, B. A. Bernevig, and J. Hu, Phys. Rev. Lett. **101**, 206404 (2008).
- [3] Q. Si and E. Abrahams, Phys. Rev. Lett. **101**, 076401 (2008).
- [4] E. Berg, S. A. Kivelson, and D. J. Scalapino, Phys. Rev. B **81**, 172504 (2010).
- [5] C. Fang *et al.*, Phys. Rev. B **77**, 224509 (2008).
- [6] C. Xu, M. Mueller, and S. Sachdev, Phys. Rev. B **78**, 02051 (2008).
- [7] K. Haule and G. Kotliar, New Journal of Physics **11**, 025021 (2009).
- [8] K. Haule, J. H. Shim, and G. Kotliar, Phys. Rev. Lett **100**, 226402 (2008).
- [9] J. Dai, Q. Si, J.-X. Zhu, and E. Abrahams, PNAS **106**, 4118 (2009).
- [10] I. I. Mazin, *et al*, Phys. Rev. Lett. **101**, 057003 (2008).
- [11] K. Kuroki *et al.*, Phys. Rev. Lett. **101**, 087004 (2008).

- [12] F. Wang *et al.*, Phys. Rev. Lett. **102**, 1047005 (2009).
- [13] R. Thomale, C. Platt, W. Hanke, and B. A. Bernevig, arXiv:1002.3599 (unpublished).
- [14] V. Cvetkovic and Z. Tesanovic, Europhys. Lett. **85**, 37002 (2009).
- [15] M. M. Korshunov and I. Eremin, Phys. Rev. B **78**, 140509 (2008).
- [16] A. V. Chubukov, D. V. Efremov, and I. Eremin, Phys. Rev. B **78**, 134512 (2008).
- [17] D. J. Scalapino, Phys. Rep. **250**, 329 (1995).
- [18] D. J. Scalapino and S. A. Trugman, Philos. Mag. B **74**, 607 (1996).
- [19] W.-F. Tsai and S. A. Kivelson, Phys. Rev. B **73**, 214510 (2006).
- [20] H. Yao, W.-F. Tsai, and S. A. Kivelson, Phys. Rev. B **76**, 161104(R) (2007).
- [21] E. Altman and A. Auerbach, Phys. Rev. B **65**, 104508 (2002).
- [22] C. de la Cruz *et al.*, Nature **453**, 899 (2008).
- [23] J. Zhao *et al.*, Nature Physics **5**, 55 (2009).
- [24] J. Zhao *et al.*, Phys. Rev. Lett. **101**, 167203 (2008).
- [25] H. Ding *et al.*, Europhys. Lett. **83**, 47001 (2008).
- [26] Y. Zhang *et al.*, Phys. Rev. Lett. **105**, (2010).
- [27] K. Nakayama *et al.*, arXiv:1009.4236 (2010).
- [28] S. Raghu *et al.*, Phys. Rev. B **77**, 22503 (2008).
- [29] M. Daghofer, *et al.*, Phys. Rev. B **81**, 014511 (2010).
- [30] M. Daghofer *et al.*, Phys. Rev. Lett **101**, 237004 (2008).
- [31] D. Fisher and P. C. Hohenberg, Phys. Rev. B **37**, 493 (1988).
- [32] P. A. Lee and X.-G. Wen, Phys. Rev. B **78**, 144517 (2008).
- [33] W. C. Lee, S. C. Zhang, and C. Wu, Phys. Rev. Lett **102**, 217002 (2009).
- [34] P. Goswami, P. Nikolic, and Q. Si, Europhys. Lett. **91**, 37006 (2010).
- [35] Y. Zhang *et al.*, arXiv:0904.4022 (2009).